U-Pb Ages, Geochemistry and Pb-Isotopic Compositions of Jurassic Intrusions, and Associated Au(-Cu) Skarn Mineralization, in the Southern Quesnel Terrane, Southern British Columbia (NTS 082E, F, L, 092H, I)

J.K. Mortensen, University of British Columbia, Vancouver, BC, jmortensen@eos.ubc.ca

Mortensen, J.K. (2014): U-Pb ages, geochemistry and Pb-isotopic compositions of Jurassic intrusions, and associated Au(-Cu) skarn mineralization, in the southern Quesnel terrane, southern British Columbia (NTS 082E, F, L, 092H, I); *in* Geoscience BC Summary of Activities 2013, Report 2014-1, p. 83–98.

Introduction

Mesozoic and Cenozoic intrusive rocks constitute a major component of the Quesnel terrane in southern British Columbia (Figure 1). Early and Middle Jurassic intrusions in this region are of particular interest because of their inferred linkages with a variety of styles of intrusion-related mineralization. World-class Au and Au-Cu skarns that are interpreted as being temporally and genetically related to Jurassic intrusions in the region include the Nickel Plate mine in the Hedley–Apex Mountain area, which produced a total of 71 tonnes of gold from 13.4 million tonnes of ore (Ray et al., 1996), and the Phoenix mine in the Greenwood area, which produced 28.3 tonnes of gold and 235.7 tonnes of copper from 13.1 million tonnes of ore (Figure 1; MINFILE 082ESE020; BC Geological Survey, 2013). In addition, the currently operating Buckhorn Mountain (Crown Jewel) mine, located ~5 km south of the BC-Washington border and approximately 28 km west-southwest of Greenwood (Figure 1), is a Au-bearing skarn deposit, with past production and current resources of 30.1 tonnes of gold, that is also associated with Jurassic intrusive rocks (Scorrar, 2012). Despite the clear economic significance of Jurassic intrusions and their associated mineralization in this region, these bodies have been the subject of relatively little detailed study. An investigation of Jurassic intrusive rocks between Hedley and Osoyoos was undertaken as part of a larger study of Paleozoic basement rocks and superimposed Mesozoic magmatism in the southern Quesnel terrane (Mortensen et al., 2011). Locations and brief lithological descriptions of the samples that were included in this study are given in Table 1. Uranium-lead zircon ages are reported here for a total of eight intrusions. The geochemical compositions of these bodies are also compared with Early and Middle Jurassic intrusions in the Greenwood area (Boundary Creek mineral district) and the Buckhorn Mountain area in northern Washington. In addition, Pb-isotopic compositions are reported for all of the intrusive rocks and for Au-Cu skarn mineralization from the areas of the Nickel Plate and Phoenix mines. The implications of these results are discussed in terms of constraints on the tectonic evolution of the region and the age(s) of the Au-Cu skarns present.

Keywords: *Quesnel terrane, Jurassic intrusions, Au-Cu skarn, U-Pb geochronology, Pb isotopes, lithogeochemistry*

This publication is also available, free of charge, as colour digital files in Adobe Acrobat® PDF format from the Geoscience BC website: http://www.geosciencebc.com/s/DataReleases.asp.

Regional Geology

The basement of the southern Quesnel terrane in southern BC comprises a variety of metamorphosed volcanic and sedimentary assemblages of middle and late Paleozoic age (Figure 1). These assemblages are unconformably overlain by mainly Late Triassic volcanic, clastic and carbonate rocks of the Nicola Group, and have been subsequently intruded by several suites of Jurassic, Cretaceous and Paleogene plutons (Figure 1). Middle Jurassic and mid-Cretaceous volcanic rocks are also present, particularly in the region west of Osoyoos. Paleogene volcanic and sedimentary rocks, commonly closely associated with high-level intrusions, occur throughout the region.

Geology of the Hedley–Apex Mountain Area

The Hedley–Apex Mountain area (Figure 2) is underlain by metasedimentary and mafic metavolcanic rocks of the Apex Mountain Complex of Ray and Dawson (1994; comprising parts of the Independence, Bradshaw, Old Tom and Shoemaker assemblages of Bostock, 1940). The overlying Nicola Group strata in this area are dominantly sedimentary, and have been subdivided into at least six separate rock units (Oregon Claims, French Mine, Hedley, Chuchuwayha, Stemwinder and Whistle formations) by Ray and Dawson (1994) and Ray et al. (1996) based on lithofacies and, to some extent, on fossil ages. These authors also identified five distinct intrusive phases of known or inferred Jurassic ages in the area that they interpreted as representing two separate pulses of magmatism. These intrusive units were distinguished based on modal composition and on a limited number of relatively imprecise U-Pb and K-Ar crystallization ages. The Hedley intrusions, which consist of several irregular stocks (Aberdeen, Stemwinder and Toronto) and a very large number of sills and dikes within the Nicola Group units (Figure 2), were interpreted as the old-

Table 1. Locations and brief lithological descriptions of samples used in the study.

Sample no.	Rock unit	Lithology	Location	UTM		Datum
				Easting	Northing	
10-M-04	Bromley batholith	Hornblende granodiorite	Road west from Apex Mountain resort	288431	5476152	NAD27
10-M-05	Lookout Mtn. pluton	Biotote-hornblende quartz monzonite	Logging road west of Nickle Plate Lake	284467	5475953	NAD27
10-M-06	Offshoot of Toronto stock	Fine- to medium-grained diorite	Old access road toward Nickle Plate mine	714559	5471320	NAD27
10-M-07	Offshoot of Toronto stock	Fine- to medium-grained diorite	Old access road toward Nickle Plate mine	714828	5471134	NAD27
10-M-08	Cahill Creek Stock	Biotite quartz monzonite	Main road from Hedley up to Mascot mine	715091	5468977	NAD27
10-M-10	Olalla pluton	Massive syenite	Road up Olalla Creek	292745	5461717	NAD83
10-M-33	Mt Riordan pluton	Massive quartz diorite	Road on west side of Apex Mountain resort	287928	5476012	NAD27
10KL-111	Kruger syenite	Coarse-grained syenite	Roadcut on north side of Highway 3	304934	5432930	NAD27
10KL-115	Bromley batholith?	Hornblende granodiorite	East side of Apex Mountain resort access road	289672	5475444	NAD27

est plutons in the area. The Hedley intrusions are metaluminous and predominantly mafic to intermediate in composition (gabbro to diorite). Four younger intrusive phases, of mainly intermediate composition, are also recognized; these include eastern extensions of the Bromley batholith, as well as the Lookout Ridge pluton, the Mount Riordan stock and the Cahill Creek pluton (Figure 2). Isotopic-age determinations reported by Ray and Dawson (1994) indicated that crystallization ages for these units that ranged from ca. 194 to 168 Ma. Middle Jurassic subaerial volcanic rocks of the Skwel Peken formation overlie the Nicola Group strata in a small area ~2 km north of the Nickel Plate mine, and a variety of mainly felsic dikes and plugs of uncertain age crosscut most rock units in the area.

Skarn Au(±Cu) mineralization in the Hedley–Apex Mountain area is mainly developed within limestone of the French Mine formation and calcareous siltstone of the Hedley Formation. Skarn development is most prominent where

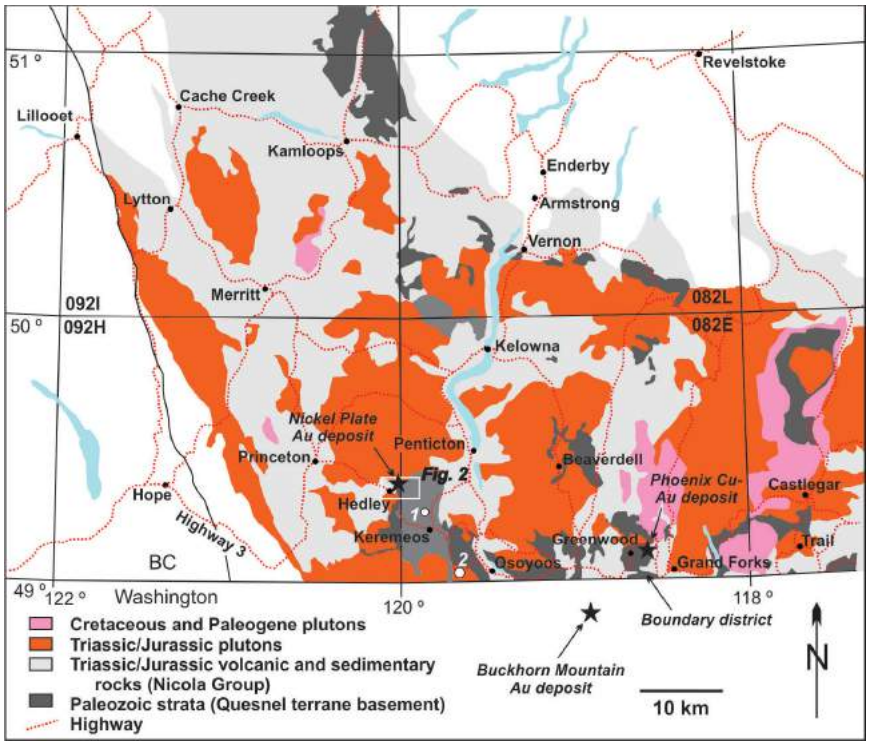

Figure 1. Distribution of Paleozoic basement units and Early and Late Mesozoic intrusions in the Quesnel terrane of southern and south-central British Columbia. Star outside the map border shows the location of the Buckhorn Mountain (Crown Jewel) Au-bearing skarn deposit. Location of Figure 2 is shown as the white box. White circles marked 1 and 2 are the locations of the Olalla pluton and Kruger syenite, respectively.

these units are cut by Hedley intrusions, and Ettlinger et al. (1992) and Ray et al. (1996) suggested that this close association provides evidence that the Hedley intrusions were likely the main causative intrusions responsible for skarn formation in this area.

U-Pb Geochronology

Individual samples weighing from 5–10 kg each were collected from surface exposures from eight different plutons. Zircons were separated from the samples through conventional crushing and grinding operations, and using Wilfley table, heavy liquids and Frantz magnetic-separator techniques. Zircons were analyzed by laser-ablation multiple-collector inductively coupled plasma–mass spectrometry (LA-MC-ICP-MS) at the Pacific Centre for Isotopic and Geochemical Research, University of British Columbia, Vancouver, BC. The methodology for zircon selection, mounting and analysis for the U-Pb age determinations by LA-MC-ICP-MS are as described by Tafti et al. (2009) and Beranek and Mortensen (2011). Zircons recovered from the various samples typically comprised stubby to elongated euhedral prisms with no evidence for inherited cores. Twenty zircon grains were analyzed from most of the samples, except for the Olalla pluton sample, which yielded only nine zircon grains of sufficiently high quality for analysis. Analytical results are presented in Table 2 and are shown graphically in Figures 3 and 4. The individual data sets are interpreted below.

Sample 10M-06 (Toronto Stock)

A sample of fine- to medium-grained hornblende diorite was collected from a sill ~3 m thick near the southern edge of the Toronto stock (Figure 2). A total of twenty zircon grains were analyzed (Table 2; Figure 3a, b). All of the analyses were concordant and fifteen grains yielded a calculated weighted-average $^{206}Pb/^{238}U$ age of 195.5 ±1.2 Ma (mean square of weighted deviates [MSWD] = 0.27; probability of fit = 1.0), which is interpreted as the crystallization age of the sample. Five grains gave a cluster of slightly older ages (average of ca. 202 Ma) that appears to represent a distinct and separate population from the other analyses. These grains are interpreted as xenocrysts that were incorporated into the magma, possibly entrained from Late Triassic Nicola Group units, and the five analyses were excluded from the final calculation of the crystallization age of the sample.

Sample 10M-04 (Bromley Batholith)

Twenty zircon grains were analyzed from a sample of very fresh hornblende granodiorite from the Bromley batholith, located north of the Apex Mountain ski resort (Figure 2). All analyses were concordant and eighteen analyses

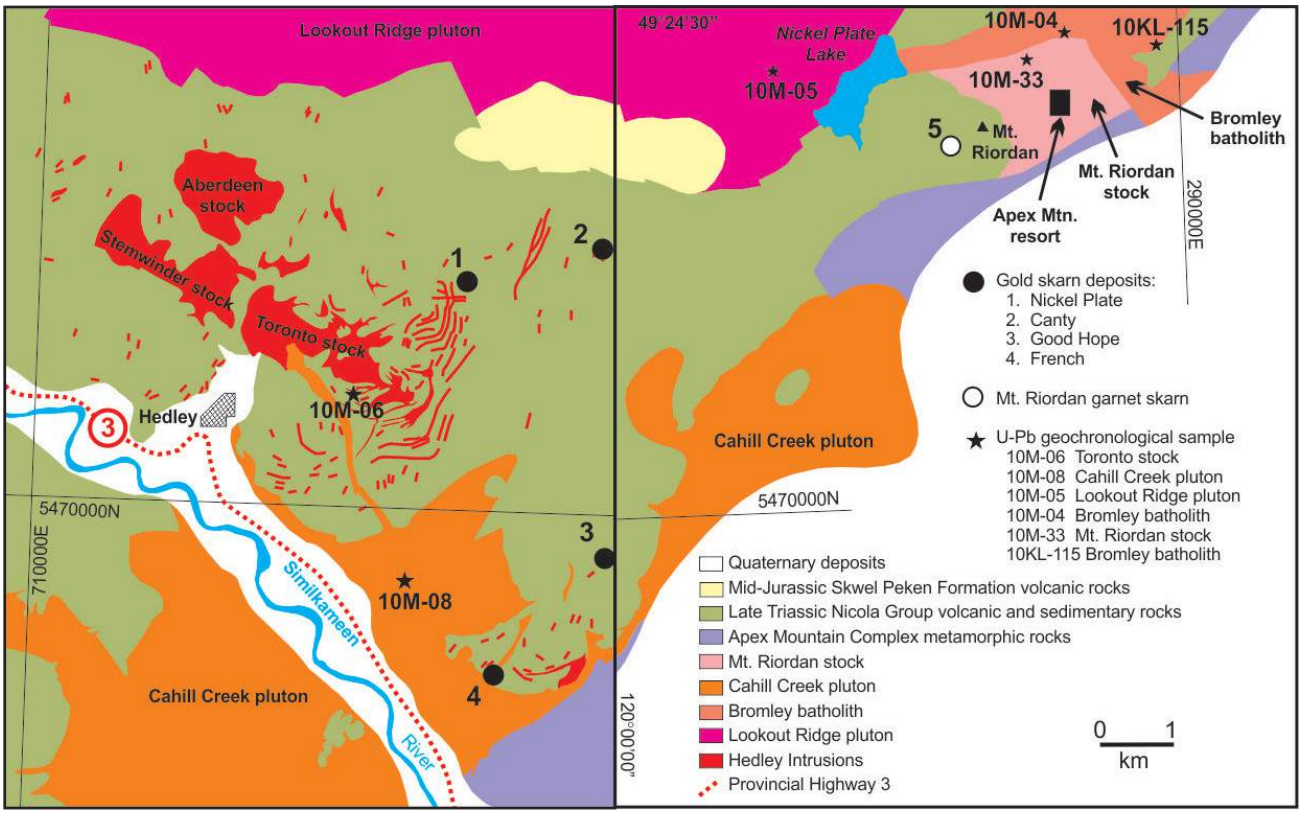

Figure 2. Simplified geology of the Hedley–Apex Mountain area (modified from Ray and Dawson, 1994). Locations of samples of the Olalla pluton and Kruger syenite are not shown on the map.

Table 2. Results of U-Pb zircon analyses for intrusive rock units from the Hedley–Apex Mountain area. Analyses by Pacific Centre for Isotopic and Geochemical Research, University of British Columbia, Vancouver, BC.

Fraction	Isotopic ratios							Isotopic ages (Ma)						Background corrected mean counts per second at specified mass							
	$^{207}Pb/^{235}U$	1σ (%)	$^{206}Pb/^{238}U$	1σ (%)	ρ	$^{207}Pb/^{206}Pb$	1σ (%)	$^{207}Pb/^{235}U$	1σ	$^{206}Pb/^{238}U$	1σ	$^{207}Pb/^{206}Pb$	1σ	202	204	206	207	208	232	235	238
Sample 10M-06 (Toronto stock; 714559E, 5471664N, NAD83)																					
1	0.20796	0.0052	0.03058	0.00027	0.35	0.04889	0.00117	191.8	4.4	194.2	1.7	142.5	55.2	9	2	8605	421	541	22700	1787	269157
2	0.21696	0.00605	0.03095	0.0003	0.35	0.04922	0.00131	199.4	5.1	196.5	1.9	158.5	61.0	31	23	9390	463	617	26929	1886	290553
3	0.22136	0.00638	0.03185	0.00033	0.36	0.05162	0.00142	203.0	5.3	202.1	2.0	268.4	61.7	18	19	7382	382	429	18158	1526	222278
4	0.20916	0.00659	0.03099	0.00034	0.35	0.04887	0.00147	192.8	5.5	196.8	2.1	141.6	69.1	14	0	6049	297	332	13686	1255	187344
5	0.22095	0.00547	0.03181	0.00028	0.36	0.04933	0.00115	202.7	4.6	201.9	1.7	163.4	53.4	32	19	16726	829	1273	53732	3321	505183
6	0.21032	0.00699	0.03093	0.00035	0.34	0.04938	0.00155	193.8	5.9	196.4	2.2	166.1	71.9	19	23	4926	244	493	20696	1031	153324
7	0.2134	0.00594	0.03083	0.0003	0.35	0.04896	0.00127	196.4	5.0	195.7	1.9	146.0	59.8	0	16	8228	405	582	25287	1685	257205
8	0.21289	0.00998	0.03075	0.0005	0.35	0.04872	0.00217	196.0	8.4	195.3	3.1	134.3	101.5	3	21	5427	266	403	16279	1110	170194
9	0.21229	0.00669	0.03091	0.00034	0.35	0.04917	0.00144	195.5	5.6	196.2	2.1	156.0	67.2	0	14	9203	456	573	23208	1907	287345
10	0.21168	0.00724	0.03031	0.00036	0.35	0.05028	0.0016	195.0	6.1	192.5	2.3	208.1	72.2	9	0	9358	474	652	27615	1990	298228
11	0.21202	0.00759	0.03083	0.00038	0.34	0.04937	0.00163	195.3	6.4	195.7	2.4	165.5	75.4	28	8	11798	587	998	41708	2463	370120
12	0.22278	0.01178	0.03202	0.00058	0.34	0.04906	0.00244	204.2	9.8	203.2	3.6	150.8	112.6	6	0	3233	160	414	16679	638	97715
13	0.22375	0.02117	0.03233	0.00106	0.35	0.04931	0.00445	205.0	17.6	205.1	6.6	162.8	198.1	0	23	2253	112	195	8002	445	67480
14	0.22048	0.01007	0.03211	0.00051	0.35	0.04974	0.0021	202.3	8.4	203.7	3.2	182.6	95.6	0	0	7610	381	553	21729	1541	229601
15	0.20669	0.0078	0.0308	0.0004	0.34	0.04853	0.00165	190.8	6.6	195.6	2.5	125.3	78.3	19	1	12797	626	1071	46388	2698	402607
16	0.2136	0.0106	0.03102	0.00053	0.34	0.05041	0.0023	196.6	8.9	196.9	3.3	214.1	102.3	0	3	13872	705	998	44206	2940	433668
17	0.2123	0.01073	0.03063	0.00053	0.34	0.04933	0.00229	195.5	9.0	194.5	3.3	163.7	104.9	8	5	7658	381	452	20234	1597	242474
18	0.21226	0.01236	0.03097	0.00062	0.34	0.04908	0.00264	195.4	10.4	196.6	3.9	151.7	121.5	0	1	7182	355	480	18819	1490	224961
19	0.21209	0.01162	0.03063	0.00058	0.35	0.04996	0.0025	195.3	9.7	194.5	3.6	193.1	112.6	29	15	5430	273	440	17448	1148	172057
20	0.21189	0.01382	0.03093	0.0007	0.35	0.05076	0.00307	195.1	11.6	196.4	4.4	230.1	133.8	0	0	4131	211	381	14412	887	129587
Sample 10M-04 (Bromley batholith; 288431E, 5476152E, NAD83)																					
1	0.20873	0.00814	0.0306	0.00042	0.35	0.04882	0.00183	192.5	6.8	194.3	2.6	139.0	85.9	20	0	3800	189	268	11128	774	119464
2	0.19739	0.00712	0.03027	0.00038	0.35	0.04685	0.00163	182.9	6.0	192.3	2.4	41.3	81.4	10	0	7207	344	780	28976	1491	229041
3	0.2017	0.00537	0.03069	0.00028	0.34	0.04722	0.00121	186.6	4.5	194.9	1.8	59.9	60.6	1	1	6043	290	413	15916	1233	189433
4	0.21345	0.00348	0.03061	0.00019	0.38	0.05121	0.0008	196.4	2.9	194.3	1.2	250.2	35.7	21	24	13310	694	993	41248	2785	418411
5	0.20703	0.00499	0.03059	0.00025	0.34	0.04816	0.00112	191.1	4.2	194.3	1.6	107.2	54.0	10	21	5832	286	481	19796	1183	183417
6	0.21068	0.01258	0.03107	0.00062	0.33	0.04729	0.00272	194.1	10.6	197.2	3.9	63.5	131.9	24	8	3834	184	275	11400	751	118777
7	0.20857	0.00708	0.03014	0.00036	0.35	0.05076	0.00167	192.4	6.0	191.4	2.3	229.9	74.1	21	13	3528	182	426	16320	750	112676
8	0.20743	0.00615	0.03052	0.00032	0.35	0.0483	0.00138	191.4	5.2	193.8	2.0	114.0	66.1	33	0	4318	212	478	19861	878	136173
9	0.21526	0.00545	0.03057	0.00027	0.35	0.05048	0.00123	198.0	4.6	194.1	1.7	216.9	55.5	8	4	4980	255	592	24554	1020	156782
10	0.21547	0.00777	0.03066	0.00038	0.34	0.04931	0.00171	198.1	6.5	194.7	2.4	162.8	79.1	15	3	3603	180	368	15194	721	113114
11	0.21167	0.00913	0.03093	0.00045	0.34	0.04845	0.00201	195.0	7.7	196.4	2.8	121.3	95.0	0	0	3806	187	336	13923	762	118477
12	0.20649	0.00978	0.03025	0.0005	0.35	0.04956	0.00227	190.6	8.2	192.1	3.1	174.4	103.3	0	0	4470	225	276	12006	938	142272
13	0.22367	0.00877	0.03193	0.00044	0.35	0.04884	0.00183	205.0	7.3	202.6	2.7	140.2	85.8	50	36	6586	326	424	17817	1259	198640
14	0.20968	0.00754	0.03069	0.00038	0.34	0.04913	0.00171	193.3	6.3	194.9	2.4	154.0	79.4	21	18	3988	198	255	11361	818	125162
15	0.21355	0.00503	0.03121	0.00025	0.34	0.04941	0.00112	196.5	4.2	198.1	1.6	167.3	52.2	30	13	6045	303	396	16995	1225	186535
16	0.20799	0.01099	0.03025	0.00057	0.36	0.05136	0.00262	191.9	9.2	192.1	3.6	256.9	113.2	0	0	5331	277	387	15087	1153	169795
17	0.20756	0.00557	0.0305	0.00028	0.34	0.04893	0.00127	191.5	4.7	193.7	1.8	144.5	59.6	75	8	5366	266	436	20034	1109	169470
18	0.21177	0.00848	0.03061	0.00042	0.34	0.0482	0.00185	195.0	7.1	194.3	2.7	109.1	88.4	26	12	4166	203	312	11764	831	131128
19	0.21077	0.00722	0.03084	0.00037	0.35	0.05036	0.00167	194.2	6.1	195.8	2.3	211.8	74.9	0	2	4972	253	335	13542	1042	155376
20	0.2057	0.00454	0.02947	0.00023	0.35	0.05034	0.00107	189.9	3.8	187.3	1.5	210.9	48.7	0	3	6549	333	734	29903	1406	214111
Sample 10KL-115 (Bromley batholith; 289672E, 5475444N, NAD83)																					
1	0.22543	0.04781	0.03246	0.0018	0.26	0.049	0.01023	206.4	39.6	205.9	11.2	148.0	427.5	0	16	304	14	39	1355	66	10185
2	0.20404	0.04593	0.02953	0.00182	0.27	0.05397	0.01208	188.5	38.7	187.6	11.4	369.7	438.2	14	1	283	15	11	648	75	10406
3	0.20615	0.02549	0.0304	0.00126	0.34	0.05232	0.00632	190.3	21.5	193.1	7.9	299.5	254.5	0	0	990	51	115	4498	252	35361
4	0.18863	0.06364	0.03036	0.00226	0.22	0.05208	0.01748	175.5	54.4	192.8	14.1	288.8	626.4	0	0	192	9	17	668	53	6865
5	0.24766	0.046	0.03074	0.00199	0.35	0.06599	0.0121	224.7	37.4	195.2	12.4	806.1	343.2	18	0	307	20	37	827	82	10855

Table 2 (continued)

Fraction	Isotopic ratios							Isotopic ages (Ma)						Background corrected mean counts per second at specified mass							
	$^{207}Pb/^{235}U$	1σ (%)	$^{206}Pb/^{238}U$	1σ (%)	ρ	$^{207}Pb/^{206}Pb$	1σ (%)	$^{207}Pb/^{235}U$	1σ	$^{206}Pb/^{238}U$	1σ	$^{207}Pb/^{206}Pb$	1σ	202	204	206	207	208	232	235	238
6	0.20426	0.0937	0.03085	0.00302	0.21	0.04359	0.01977	188.7	79.0	195.9	18.9	0.1	720.0	0	9	158	6	1	307	33	5576
7	0.288	0.03881	0.03215	0.00147	0.34	0.06822	0.00896	257.0	30.6	204.0	9.2	875.3	250.5	0	21	308	20	23	701	73	10414
8	0.18482	0.02585	0.03072	0.00121	0.28	0.05063	0.007	172.2	22.2	195.0	7.6	224.0	291.3	0	0	452	22	55	1661	124	15987
9	0.20088	0.24106	0.03103	0.00472	0.13	0.03699	0.04423	185.9	203.8	197.0	29.5	0.1	1226.5	0	11	63	2	19	190	11	2227
10	0.21915	0.09059	0.03077	0.00262	0.21	0.06227	0.0258	201.2	75.5	195.4	16.4	683.5	700.6	0	0	92	5	6	291	26	3278
11	0.20521	0.06674	0.02932	0.00181	0.19	0.04419	0.01426	189.5	56.2	186.3	11.3	0.1	546.7	0	3	240	10	25	821	52	8918
12	0.23902	0.04671	0.03392	0.00172	0.26	0.05139	0.00985	217.6	38.3	215.0	10.7	258.5	389.2	0	0	368	18	18	813	79	11794
13	0.21293	0.05366	0.03116	0.00198	0.25	0.04511	0.0112	196.0	44.9	197.8	12.4	0.1	463.5	0	8	299	13	19	1020	63	10452
14	0.19398	0.03959	0.03108	0.00137	0.22	0.0444	0.00896	180.0	33.7	197.3	8.6	0.1	343.8	0	0	372	16	21	145	85	13021
15	0.19438	0.06127	0.03132	0.00299	0.30	0.05067	0.01583	180.4	52.1	198.8	18.7	225.7	596.2	48	0	240	12	31	733	62	8352
16	0.12909	0.01652	0.01623	0.00069	0.33	0.05579	0.00717	123.3	14.9	103.8	4.4	443.9	263.2	0	2	583	32	158	14391	253	39128
17	0.08308	0.01724	0.01722	0.00071	0.20	0.03719	0.00773	81.0	16.2	110.1	4.5	0.1	0.0	50	23	339	12	143	12116	152	21442
18	0.19269	0.02835	0.03061	0.00109	0.24	0.04344	0.00629	178.9	24.1	194.4	6.8	0.1	182.1	0	2	454	19	66	2108	102	16155
19	0.21169	0.03525	0.03102	0.0016	0.31	0.04669	0.00757	195.0	29.5	196.9	10.0	33.1	348.5	0	0	856	40	78	2769	189	30032
Sample 10M-05 (Lookout Ridge pluton; 284467E, 5475953N, NAD83)																					
1	0.21877	0.0049	0.03184	0.00025	0.35	0.04948	0.00107	200.9	4.1	202.0	1.5	170.7	49.5	1	17	7395	370	450	21027	1479	249564
2	0.21915	0.0056	0.03181	0.00029	0.36	0.05029	0.00123	201.2	4.7	201.9	1.8	208.2	56.0	15	16	10295	524	693	28646	2089	347422
3	0.22218	0.00529	0.03195	0.00028	0.37	0.05099	0.00116	203.7	4.4	202.7	1.7	240.5	51.7	24	0	13909	718	1205	53152	2822	466835
4	0.21625	0.0054	0.03116	0.00028	0.36	0.04947	0.00119	198.8	4.5	197.8	1.7	170.2	55.1	43	1	6301	315	705	32522	1274	216672
5	0.2144	0.0042	0.03103	0.00022	0.36	0.05038	0.00095	197.2	3.5	197.0	1.4	212.4	43.0	57	0	8253	420	758	37347	1713	284664
6	0.22368	0.00625	0.03216	0.00032	0.36	0.05043	0.00135	205.0	5.2	204.0	2.0	214.7	60.8	8	4	9972	508	677	31605	1985	331270
7	0.21293	0.00517	0.0313	0.00026	0.34	0.04895	0.00114	196.0	4.3	198.7	1.7	145.5	53.9	3	0	6832	338	499	23898	1387	233008
8	0.21326	0.00733	0.03082	0.00036	0.34	0.05052	0.00168	196.3	6.1	195.7	2.3	219.2	75.1	10	9	4941	252	350	16327	1033	170996
9	0.21847	0.00739	0.0318	0.00037	0.34	0.05006	0.00163	200.6	6.2	201.8	2.3	197.7	73.9	26	0	6296	318	411	17044	1273	210982
10	0.21129	0.00435	0.03103	0.00023	0.36	0.0493	0.00098	194.6	3.7	197.0	1.4	162.1	45.6	30	21	9163	456	677	31251	1886	314301
11	0.20935	0.00529	0.03105	0.00027	0.34	0.04792	0.00116	193.0	4.4	197.1	1.7	94.4	57.7	31	0	9946	480	828	37083	2008	340329
12	0.22125	0.01042	0.03196	0.00049	0.33	0.04972	0.00226	203.0	8.7	202.8	3.1	181.8	102.5	3	17	2570	128	221	9688	509	85360
13	0.20586	0.0084	0.03017	0.00039	0.32	0.04855	0.00192	190.1	7.1	191.6	2.5	126.4	90.7	19	0	2761	135	270	12131	574	97054
14	0.2212	0.00705	0.03178	0.00036	0.36	0.05199	0.00159	202.9	5.9	201.7	2.3	284.8	68.5	22	17	8757	458	649	33452	1813	291930
15	0.21676	0.00487	0.03089	0.00025	0.36	0.05048	0.00109	199.2	4.1	196.1	1.6	217.0	49.1	0	6	9196	467	720	35982	1887	315066
16	0.21727	0.00696	0.03099	0.00034	0.34	0.05008	0.00154	199.6	5.8	196.7	2.2	198.8	70.1	14	7	5647	284	351	17483	1146	192531
17	0.21517	0.00556	0.03103	0.00028	0.35	0.05008	0.00124	197.9	4.6	197.0	1.8	198.9	56.7	20	0	5916	298	514	22942	1212	201236
18	0.21906	0.00779	0.03075	0.00039	0.36	0.05043	0.00172	201.1	6.5	195.2	2.4	214.7	77.2	0	0	6031	305	425	19581	1222	206818
19	0.20955	0.00797	0.03099	0.0004	0.34	0.04713	0.00172	193.2	6.7	196.7	2.5	55.6	85.4	0	0	6480	307	551	24355	1282	220302
20	0.21243	0.00442	0.031	0.00023	0.36	0.04848	0.00097	195.6	3.7	196.8	1.4	122.8	46.4	4	0	8006	390	1030	49447	1607	271798
Sample 10M-33 (Mt. Riordan stock; 287928E, 5476012N, NAD83)																					
1	0.22027	0.00804	0.03186	0.00039	0.34	0.0481	0.00169	202.1	6.7	202.2	2.4	104.3	80.8	38	8	3815	183	342	14964	738	115658
2	0.21847	0.00853	0.03157	0.0004	0.32	0.04877	0.00183	200.6	7.1	200.4	2.5	136.6	86.1	10	0	3074	150	330	13713	608	94063
3	0.22329	0.00817	0.03153	0.0004	0.35	0.05094	0.00179	204.6	6.8	200.1	2.5	238.1	79.2	0	0	3375	172	363	13748	683	103416
4	0.21829	0.00691	0.03184	0.00034	0.34	0.04957	0.00151	200.5	5.8	202.1	2.1	175.0	69.7	0	20	3560	176	294	12226	717	108030
5	0.20879	0.00764	0.03059	0.00038	0.34	0.05008	0.00177	192.5	6.4	194.2	2.4	198.6	80.1	22	0	3108	155	258	11110	662	98188
6	0.21824	0.00988	0.03183	0.00049	0.34	0.05023	0.00219	200.4	8.2	202.0	3.1	205.7	98.2	0	0	3589	180	371	14997	734	108972
7	0.22238	0.01199	0.03162	0.00059	0.35	0.04907	0.00254	203.9	10.0	200.7	3.7	151.4	116.8	16	0	4873	239	624	25811	956	148937
8	0.21508	0.01918	0.03102	0.00097	0.35	0.05042	0.00433	197.8	16.0	196.9	6.1	214.4	187.8	0	9	3427	172	389	13864	714	106807
9	0.21034	0.0105	0.03079	0.00053	0.34	0.04878	0.00234	193.8	8.8	195.5	3.3	137.1	109.2	13	6	4027	196	368	15176	830	126411
10	0.22145	0.00854	0.0321	0.00042	0.34	0.04911	0.00182	203.1	7.1	203.7	2.6	152.9	84.5	13	0	3765	184	351	14958	742	113386
11	0.2123	0.01266	0.03071	0.00065	0.35	0.0525	0.00303	195.5	10.6	195.0	4.1	307.3	126.0	5	0	3249	170	353	12767	715	102300
12	0.20859	0.00671	0.03086	0.00034	0.34	0.04894	0.00152	192.4	5.6	195.9	2.1	145.1	71.1	18	0	4325	211	475	21074	904	135528

Table 2 (continued)

Fraction	Isotopic ratios							Isotopic ages (Ma)						Background corrected mean counts per second at specified mass							
	$^{207}Pb/^{235}U$	1σ (%)	$^{206}Pb/^{238}U$	1σ (%)	ρ	$^{207}Pb/^{206}Pb$	1σ (%)	$^{207}Pb/^{235}U$	1σ	$^{206}Pb/^{238}U$	1σ	$^{207}Pb/^{206}Pb$	1σ	202	204	206	207	208	232	235	238
13	0.2162	0.00588	0.03072	0.00029	0.35	0.05066	0.00133	198.7	4.9	195.1	1.8	225.2	59.4	27	0	5056	255	692	28289	1055	159131
14	0.20717	0.00651	0.03079	0.00031	0.32	0.04867	0.00148	191.2	5.5	195.5	2.0	132.1	70.0	51	0	4708	228	607	25619	986	147891
15	0.21562	0.0078	0.0306	0.00038	0.34	0.04984	0.00174	198.3	6.5	194.3	2.4	187.5	79.2	27	0	3262	162	338	14143	672	103086
16	0.21176	0.00753	0.03148	0.00037	0.33	0.04814	0.00165	195.0	6.3	199.8	2.3	105.9	79.0	0	30	3281	157	240	9862	665	100826
17	0.21177	0.00824	0.03064	0.0004	0.34	0.04882	0.00183	195.0	6.9	194.5	2.5	139.4	85.9	0	14	3719	180	279	10718	765	117434
18	0.21417	0.01114	0.03183	0.00056	0.34	0.04734	0.00237	197.0	9.3	202.0	3.5	65.7	115.6	0	0	3232	152	298	13975	637	98248
19	0.22087	0.00923	0.03181	0.00045	0.34	0.0495	0.00199	202.6	7.7	201.9	2.8	171.4	91.1	0	9	3939	193	396	15786	788	119797
20	0.21805	0.01728	0.03204	0.00086	0.34	0.0486	0.0037	200.3	14.4	203.3	5.4	128.4	170.1	12	27	3550	171	388	15310	707	107216
Sample 10M-08 (Cahill Creek pluton; 715091E, 5468977N, NAD83)																					
1	0.17324	0.00692	0.02534	0.00035	0.35	0.05	0.00193	162.2	6.0	161.3	2.2	194.8	87.2	12	0	4153	209	400	23311	1075	181123
2	0.17351	0.00487	0.02538	0.00025	0.35	0.04936	0.0013	162.5	4.2	161.5	1.6	164.8	60.6	0	9	8214	408	845	49214	2096	357355
3	0.17293	0.00715	0.02541	0.00036	0.34	0.04781	0.0019	162.0	6.2	161.7	2.3	89.1	92.7	0	15	7863	378	732	41679	1950	341403
4	0.17237	0.00476	0.02547	0.00025	0.36	0.04905	0.00127	161.5	4.1	162.1	1.6	150.2	59.7	41	0	9096	449	1227	74538	2321	393611
5	0.17836	0.00816	0.02535	0.0004	0.34	0.05122	0.00227	166.6	7.0	161.4	2.5	250.9	98.6	0	6	3761	193	330	18201	968	163347
6	0.17293	0.00492	0.02564	0.00025	0.34	0.04843	0.00129	162.0	4.3	163.2	1.6	120.3	61.8	22	0	9569	465	1048	57259	2402	410242
7	0.19032	0.00683	0.02712	0.00034	0.35	0.04952	0.00169	176.9	5.8	172.5	2.1	172.7	77.7	0	7	6521	324	665	38951	1521	264097
8	0.17881	0.00781	0.02611	0.00039	0.34	0.04779	0.002	167.0	6.7	166.2	2.5	88.0	97.4	0	0	5383	258	480	29209	1289	226236
9	0.17466	0.009	0.02536	0.00045	0.34	0.05008	0.0025	163.5	7.8	161.5	2.8	198.6	112.1	0	6	3521	176	435	23949	905	152214
10	0.18461	0.00544	0.02569	0.00026	0.34	0.05141	0.00142	172.0	4.7	163.5	1.7	259.4	62.3	0	0	8488	437	1378	72879	2118	361868
11	0.17476	0.00488	0.02546	0.00025	0.35	0.04927	0.00128	163.5	4.2	162.1	1.6	160.7	59.7	18	0	11267	556	1831	102243	2846	483944
12	0.17985	0.00483	0.02588	0.00024	0.35	0.04959	0.00123	167.9	4.2	164.7	1.5	176.0	57.0	32	15	18549	921	3187	181131	4582	782926
13	0.17957	0.00738	0.02588	0.00037	0.35	0.04902	0.00193	167.7	6.4	164.7	2.3	148.8	89.6	6	19	7282	357	1179	67701	1780	307140
14	0.17637	0.00629	0.0255	0.00031	0.34	0.04877	0.00165	164.9	5.4	162.4	2.0	136.9	77.6	0	0	8536	416	953	56657	2114	365010
15	0.18583	0.00911	0.02566	0.00043	0.34	0.05148	0.00243	173.1	7.8	163.3	2.7	262.6	105.0	18	9	3282	168	536	29087	814	139368
16	0.18768	0.01321	0.02537	0.00062	0.35	0.0551	0.00378	174.6	11.3	161.5	3.9	416.0	146.6	48	0	1748	96	167	8985	459	74975
17	0.17668	0.00811	0.02569	0.00039	0.33	0.04914	0.00217	165.2	7.0	163.5	2.5	154.5	100.3	13	0	2614	128	202	11246	651	110602
18	0.17716	0.00658	0.0255	0.00032	0.34	0.05033	0.00178	165.6	5.7	162.3	2.0	210.5	79.8	2	25	4154	208	454	24469	1056	176890
19	0.18436	0.01092	0.02661	0.00054	0.34	0.04986	0.00285	171.8	9.4	169.3	3.4	188.3	128.0	0	0	2743	136	268	14739	664	111823
20	0.18513	0.00641	0.02559	0.00031	0.35	0.05125	0.00167	172.5	5.5	162.9	1.9	251.9	73.1	22	23	8485	433	817	49202	2102	359408
Sample 10M-10 (Olalla pluton; 292745E, 5461717N, NAD83)																					
1	0.20892	0.02715	0.03052	0.00139	0.35	0.05099	0.00644	192.6	22.8	193.8	8.7	240.3	267.5	0	18	1469	76	498	20992	359	52436
2	0.26407	0.05095	0.03071	0.00204	0.34	0.05773	0.01078	237.9	40.9	195.0	12.7	519.4	364.8	11	0	529	31	85	4368	116	18799
3	0.18801	0.01254	0.03066	0.00071	0.35	0.04493	0.00285	174.9	10.7	194.7	4.4	0.1	87.2	0	15	6065	279	1147	52762	1452	215524
4	0.22635	0.0181	0.03048	0.00083	0.34	0.04954	0.00378	207.2	15.0	193.6	5.2	173.5	169.0	24	11	2221	113	895	43239	487	79420
5	0.19662	0.01017	0.03045	0.00055	0.35	0.04776	0.0023	182.3	8.6	193.4	3.5	86.5	111.4	0	38	16240	799	5658	262414	3953	581328
6	0.20922	0.01141	0.03007	0.00058	0.35	0.04874	0.00248	192.9	9.6	191.0	3.6	135.5	115.5	0	4	8173	411	2755	118889	1908	296338
7	0.20902	0.01412	0.03028	0.00069	0.34	0.04955	0.00319	192.7	11.9	192.3	4.3	174.0	143.4	46	0	2096	107	261	13126	498	75510
8	0.20711	0.01048	0.0303	0.00054	0.35	0.05036	0.00236	191.1	8.8	192.4	3.4	211.4	105.1	38	17	11093	579	3408	161514	2702	399334
9	0.21098	0.01509	0.03033	0.00074	0.34	0.05041	0.00344	194.4	12.7	192.6	4.7	213.8	150.5	0	7	2341	122	353	16980	560	84215
Sample 10KL-111 (Kruger syenite; 304934E, 5432930N, NAD83)																					
1	0.18199	0.00523	0.02677	0.00027	0.35	0.04954	0.00139	169.8	4.5	170.3	1.7	173.4	64.2	5	19	3951	197	580	28755	945	142287
2	0.18258	0.00644	0.02672	0.00031	0.33	0.04796	0.00165	170.3	5.5	170.0	2.0	96.2	80.7	21	5	4075	197	741	37799	941	147045
3	0.18243	0.00378	0.02657	0.0002	0.36	0.04993	0.00101	170.2	3.2	169.1	1.2	191.7	46.3	29	19	8064	406	1289	63384	1941	292547
4	0.18684	0.00807	0.02684	0.0004	0.35	0.05024	0.00212	173.9	6.9	170.8	2.5	206.3	94.9	0	10	3117	158	452	22334	737	111983
5	0.17319	0.00292	0.02662	0.00016	0.36	0.04723	0.00078	162.2	2.5	169.3	1.0	60.6	38.0	11	15	14393	686	2242	115348	3455	521423
6	0.17731	0.00351	0.02526	0.00018	0.36	0.05074	0.00098	165.7	3.0	160.8	1.2	228.8	44.1	22	11	9731	498	1773	92346	2452	371493
7	0.18554	0.00353	0.02659	0.00018	0.36	0.04964	0.00092	172.8	3.0	169.2	1.2	178.3	42.5	2	12	9571	479	1205	62601	2256	347130

Table 2 (continued)

Fraction	Isotopic ratios							Isotopic ages (Ma)						Background corrected mean counts per second at specified mass							
	$^{207}Pb/^{235}U$	1σ (%)	$^{206}Pb/^{238}U$	1σ (%)	ρ	$^{207}Pb/^{206}Pb$	1σ (%)	$^{207}Pb/^{235}U$	1σ	$^{206}Pb/^{238}U$	1σ	$^{207}Pb/^{206}Pb$	1σ	202	204	206	207	208	232	235	238
8	0.18389	0.00409	0.02665	0.00021	0.35	0.04937	0.00107	171.4	3.5	169.5	1.3	165.3	49.9	57	8	6609	329	882	43630	1563	239220
9	0.1836	0.00597	0.02673	0.0003	0.35	0.04885	0.00155	171.2	5.1	170.1	1.9	140.5	72.9	0	16	4284	210	845	42806	1004	154579
10	0.18528	0.00551	0.02672	0.00028	0.35	0.0501	0.00145	172.6	4.7	170.0	1.8	199.7	66.0	82	24	5692	287	765	39231	1357	205507
11	0.17705	0.00474	0.02677	0.00025	0.35	0.0467	0.00122	165.5	4.1	170.3	1.6	33.8	60.3	87	0	8208	386	1124	56510	1910	295817
12	0.17831	0.00366	0.02672	0.0002	0.36	0.0492	0.00098	166.6	3.2	170.0	1.2	157.3	46.2	3	6	8219	407	991	50764	2002	296804
13	0.17956	0.01117	0.02629	0.00057	0.35	0.04849	0.00295	167.7	9.6	167.3	3.6	123.4	137.2	0	0	3822	186	541	25043	911	140261
14	0.18878	0.00757	0.02612	0.00038	0.36	0.05059	0.00198	175.6	6.5	166.2	2.4	222.3	87.9	0	22	7215	367	764	39837	1708	266564
15	0.17993	0.00651	0.02665	0.00034	0.35	0.05003	0.00177	168.0	5.6	169.6	2.1	196.2	80.2	29	1	4267	214	804	37934	1048	154531
16	0.18006	0.00471	0.02676	0.00025	0.36	0.04961	0.00126	168.1	4.1	170.2	1.6	177.0	58.4	0	7	9709	484	1889	97073	2365	350230
17	0.17988	0.00803	0.02663	0.00042	0.35	0.05077	0.00222	168.0	6.9	169.4	2.6	230.4	98.0	0	21	2682	136	411	19463	669	97249
18	0.18489	0.00503	0.0268	0.00025	0.34	0.04936	0.00131	172.3	4.3	170.5	1.6	165.0	60.9	0	6	4543	225	751	37458	1073	163684
19	0.18293	0.00342	0.02668	0.00018	0.36	0.0486	0.00088	170.6	2.9	169.7	1.1	128.7	42.1	32	7	9972	486	1734	85349	2345	360873
20	0.17654	0.00367	0.02674	0.0002	0.36	0.04768	0.00096	165.1	3.2	170.1	1.2	82.7	48.2	16	12	9676	463	1303	69308	2314	349392

Analyses by Pacific Centre for Isotopic and Geochemical Research, University of British Columbia, Vancouver, BC.

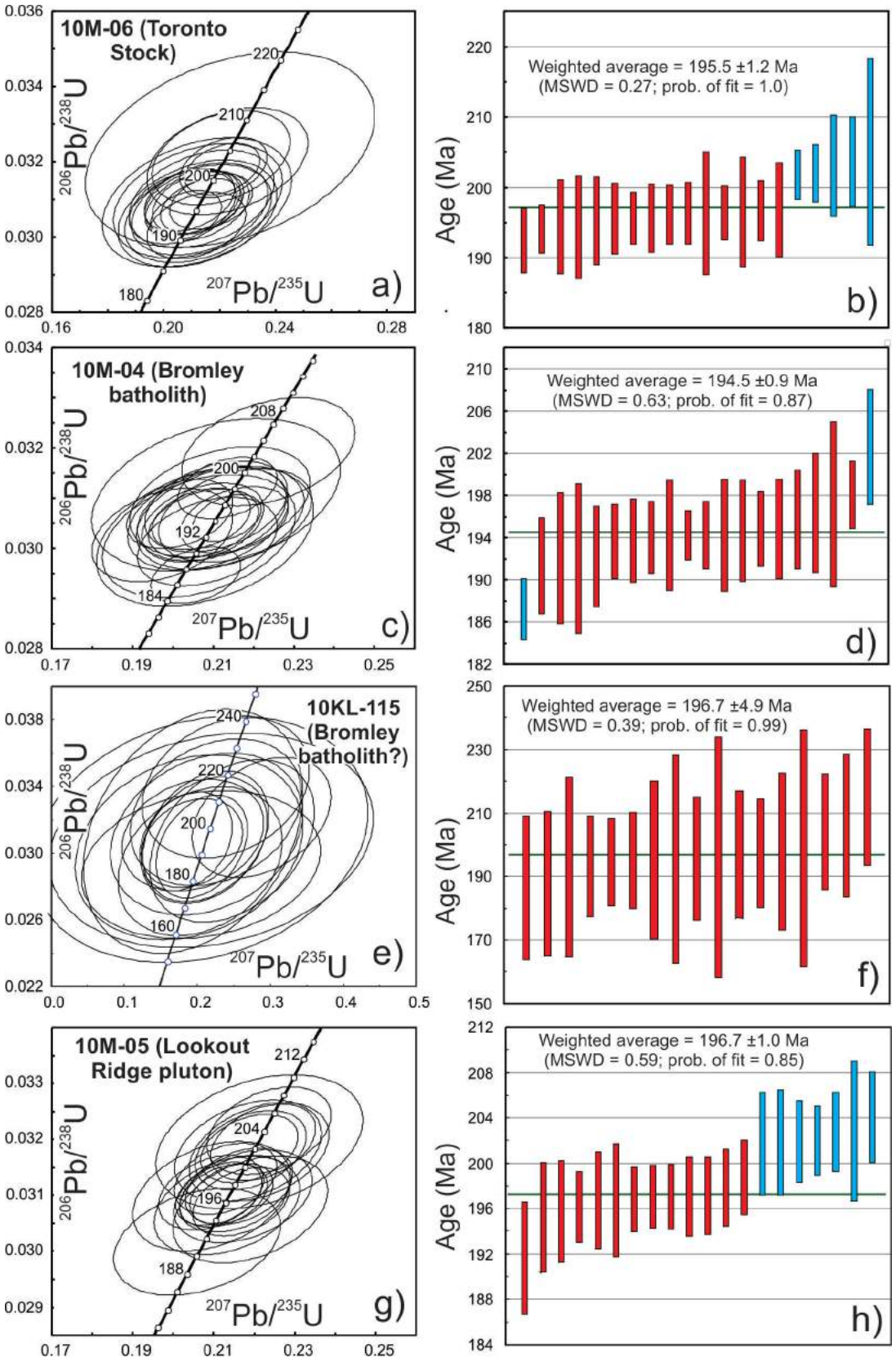

Figure 3. Conventional concordia diagrams and plots of weighted-average $^{206}Pb/^{238}U$ ages for zircons from intrusive rock units in the Hedley–Apex Mountain area (part 1). Error ellipses on concordia diagrams and weighted-average $^{206}Pb/^{238}U$ age plots are shown at the 2σ uncertainty level. Analyses shown as red bars on weighted-average age plots were used in the age calculations; those shown as blue bars were rejected.

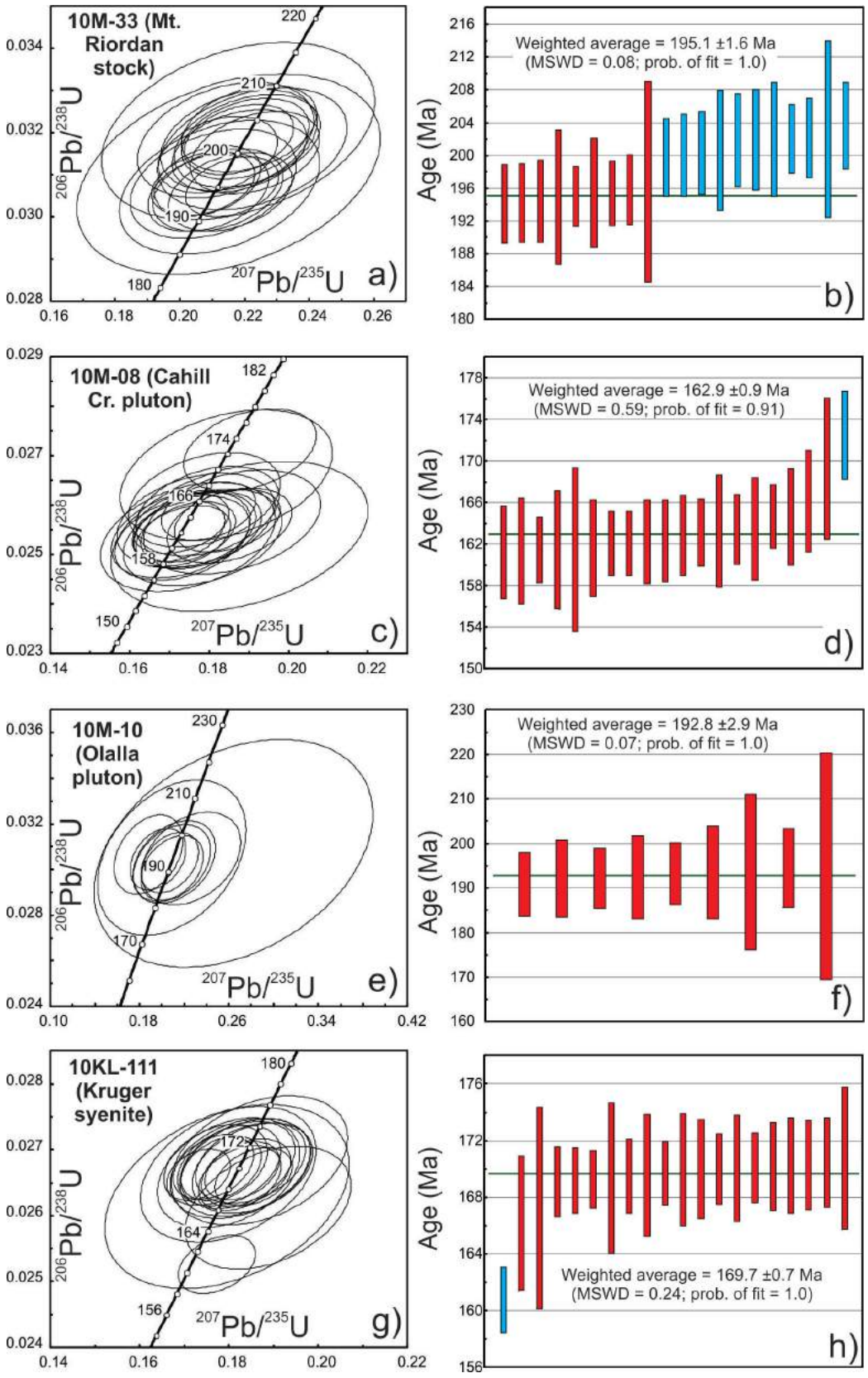

Figure 4. Conventional concordia diagrams and plots of weighted-average $^{206}Pb/^{238}U$ ages for zircons from intrusive rock units in the Hedley–Apex Mountain area (part 2). Error ellipses on concordia diagrams and weighted-average $^{206}Pb/^{238}U$ age plots are shown at the 2σ uncertainty level. Analyses shown as red bars on weighted-average age plots were used in the age calculations; those shown as blue bars were rejected.

yielded a calculated weighted-average $^{206}Pb/^{238}U$ age of 194.5 ±0.9 Ma (MSWD = 0.63; probability of fit = 0.87; Table 2, Figure 3c, d), which is interpreted as the crystallization age of the sample. One grain gave a slightly older $^{206}Pb/^{238}U$ age and is interpreted as a xenocryst, and one grain gave a younger age, reflecting the effects of minor post-crystallization Pb loss.

Sample 10KL-115 (Bromley Batholith)

A second hornblende granodiorite sample was collected from an exposure of what is interpreted as an eastern extension of the Bromley batholith, on the northern side of the Apex Mountain access road, approximately 1.25 km east of the Apex Mountain ski resort (Figure 2). The zircons from this sample were similar in appearance to those from the previous sample; however, the analyses were somewhat less precise, yielding a calculated weighted-average $^{206}Pb/^{238}U$ age of 196.7 ±4.9 Ma (MSWD = 0.39; probability of fit = 0.99; Table 2, Figure 3e, f). This rather imprecise age determination is in agreement with that obtained from the previous sample (10M-04).

Sample 10M-05 (Lookout Ridge Pluton)

Twenty zircon grains were analyzed from a sample of massive, very fresh, biotite-hornblende quartz monzonite collected from an area located northwest of Nickel Plate Lake (Figure 2). Seven grains gave a cluster of slightly older ages (average of ca. 202 Ma); however, the remaining 13 grains gave a younger cluster of ages with a calculated weighted-average $^{206}Pb/^{238}U$ age of 196.7 ±1.0 Ma (MSWD = 0.59; probability of fit = 0.85; Table 2, Figure 3g, h), which is interpreted as the crystallization age of the sample. As with the Toronto stock sample, this older cluster of ages is interpreted as reflecting the presence of a significant older xenocrystic zircon population in the sample, and these analyses were not included in the calculation of the weighted-average age for the sample.

Sample 10M-33 (Mount Riordan Stock)

A sample of medium-grained quartz diorite of the Mount Riordan stock was collected at a site located approximately 1 km northeast of the summit of Mount Riordan (Figure 2). Twenty zircon grains were analyzed (Table 2; Figure 4a, b) and the results showed two distinct clusters of ages: an older cluster gave ages of ca. 202 Ma, whereas the younger cluster of nine grains gave a calculated weighted-average $^{206}Pb/^{238}U$ age of 195.1 ±1.6 Ma (MSWD = 0.08; probability of fit = 1.0). The presence of a ca. 202 Ma population of zircons appears to be common within intrusions in this area; hence, the age calculated for the younger cluster of grains is interpreted as the crystallization age of the sample.

Sample 10M-08 (Cahill Creek Pluton)

Nineteen of twenty zircons recovered from a sample of biotite quartz monzonite of the Cahill Creek pluton, collected on the mine access road east of Hedley (Figure 2), yielded a calculated weighted-average $^{206}Pb/^{238}U$ age of 162.9 ±0.9 Ma (MSWD = 0.59; probability of fit = 0.91; Table 2, Figure 4c, d). This is interpreted as the crystallization age of the sample, and a single zircon grain that yielded a slightly older age is considered to have been a xenocryst.

Sample 10M-10 (Olalla Pluton)

Only a small amount of zircon was recovered from this sample of medium-grained trachytic syenite of the composite Olalla pluton collected along the Olalla Creek road. The nine zircons analyzed (Table 2; Figure 4e, f) gave a calculated weighted-average $^{206}Pb/^{238}U$ age of 192.8 ±2.9 Ma (MSWD = 0.07; probability of fit = 1.0), which is interpreted as the crystallization age of the sample.

Sample 10KL-111 (Kruger Syenite)

Twenty zircons were analyzed from this sample of massive, coarse-grained, biotite quartz monzonite from a roadcut on the northern side of Highway 3 (Figure 2). Nineteen of these yielded a calculated weighted-average $^{206}Pb/^{238}U$ age of 169.7 ±0.7 Ma (MSWD = 0.24; probability of fit = 1.0; Table 2, Figure 4g, h), which is interpreted as the crystallization age of the sample. One zircon is slightly discordant and gave a slightly younger age, reflecting the effects of minor postcrystallization Pb loss.

Discussion

The results of the dating study indicate that most of the intrusive rocks in the vicinity of skarn mineralization in the Hedley–Apex Mountain area, including both the Hedley intrusions and the other intrusive units that were interpreted by Ray et al. (1996) to be somewhat younger, were emplaced during the interval between ca. 197 and 195 Ma. The Cahill Creek pluton, with an emplacement age of 162.9 Ma, is confirmed to be substantially younger than the other intrusions in the area. The composite Olalla pluton, farther to the east, is slightly younger than most of the intrusions in the Hedley–Apex Mountain area, at 192.8 Ma. The Kruger syenite was expected to give an age similar to that of the Olalla pluton; however, it is actually more similar in age to the Cahill Creek pluton.

Uranium-lead zircon ages of 179.9 ±3.8 Ma and 171.6 ±2.3 Ma were reported by Massey et al. (2010) for the Greenwood stock near Greenwood and the Gidon Creek porphyry body approximately 8 km south of Greenwood, respectively, both of which are in the Boundary Creek mineral district. Three other intrusive phases in the western part of the Boundary district have also yielded Jurassic U-Pb crystallization ages; these include the Myer's Creek stock (157.0

±1.2 Ma), the Mount Baldy granodiorite (168.5 ±1.4 Ma) and the Ed James orthogneiss (187.7 ±1.4 Ma; Massey et al., 2010). The relationship between various intrusive phases and skarn Au-Cu mineralization in the Boundary district is unknown.

A number of U-Pb zircon ages have been reported by Scorrar (2012) for various intrusive phases from the vicinity of the Buckhorn Mountain (Crown Jewel) Au-bearing skarn deposit immediately south of the BC-Washington border (Figure 1). A diorite body that is interpreted as coeval with at least some of the mafic volcanic rocks near the deposit gave an age of 193.5 ±1.2 Ma; however, with the exception of much younger bodies that are Paleogene in age, most other intrusions in the area gave crystallization ages in the range of 172–165 Ma (Scorrar, 2012). Dating by the Re-Os method of molybdenite from the Buckhorn skarn deposit gave ages of 165.5 ±0.7 Ma and 162.8 ±0.7 Ma, confirming that skarn mineralization in the Buckhorn Mountain area is related to much younger intrusions than had been interpreted by Ray et al. (1996) for very similar skarn deposits in the Hedley–Apex Mountain area. This is discussed in more detail in a later section.

Igneous Geochemistry

Major, trace and rare-earth element concentrations were determined for samples of each of the rock units that were dated in this study. Data are given in Table 3 and are shown on a series of geochemical and tectonic discriminant plots in Figure 5. Results of sample analyses from Jurassic intrusive rock units in the Boundary district near Greenwood (from Massey et al., 2010) and from the Buckhorn Mountain area in northern Washington state (from Gaspar, 2005) are also shown for comparison.

Table 3. Whole-rock geochemical analyses for Early and Middle Jurassic intrusive rock units from the Hedley–Apex Mountain area.

Sample	Major elements (wt.%)										LOI	Total
	SiO_2	TiO_2	Al_2O_3	$Fe_2O_3^t$	MnO	MgO	CaO	Na_2O	K_2O	P_2O_5	(wt. %)	(wt. %)
10M-04 (Bromley batholith)	63.70	0.52	16.20	6.44	0.11	2.36	5.80	3.33	1.70	0.14	1.00	101.48
10M-05 (Lookout Ridge pluton)	72.90	0.24	14.00	2.60	0.09	0.53	1.65	3.97	4.25	0.09	0.79	101.29
10M-06 (Toronto stock)	61.40	0.53	15.35	6.55	0.12	2.81	4.88	3.71	2.25	0.14	1.11	99.07
10M-07 (Toronto stock)	57.30	0.47	18.55	6.59	0.11	3.07	8.00	4.08	0.87	0.14	1.39	100.74
10M-08 (Cahill Creek pluton)	61.20	0.64	17.30	6.40	0.13	2.03	5.41	4.15	2.29	0.23	0.98	100.95
10M-10 (Olalla pluton)	64.00	0.31	16.00	4.00	0.07	1.21	4.07	3.19	4.15	0.14	2.17	99.65
10M-33 (Mt. Riordan stock)	65.20	0.45	15.80	5.09	0.11	2.01	5.28	3.19	2.31	0.11	1.17	100.91
10KL-111 (Kruger syenite)	67.10	0.39	15.40	4.39	0.12	1.20	3.73	3.94	3.51	0.17	1.09	101.22
10KL-115 (Bromley batholith)	60.10	0.56	16.35	6.73	0.12	2.86	5.75	3.15	2.24	0.15	2.02	100.26

Sample	Trace and rare-earth elements (ppm)												
	Ba	Ce	Cr	Cs	Dy	Er	Eu	Ga	Gd	Hf	Ho	La	Lu	Nb
10M-04 (Bromley batholith)	1270	25.3	30	2.51	3	1.89	0.89	18.4	2.97	2.4	0.62	12.6	0.3	3.6
10M-05 (Lookout Ridge pluton)	1300	48.8	10	4.92	3.16	2.07	0.7	15.8	3.36	4.9	0.64	32.1	0.38	8.3
10M-06 (Toronto stock)	1535	27.4	60	4.54	2.73	1.67	0.96	18.4	3	2.9	0.57	13.9	0.25	3.6
10M-07 (Toronto stock)	892	14.9	30	3.98	1.97	1.19	0.78	18.5	2.14	1.3	0.4	7.2	0.17	1.6
10M-08 (Cahill Creek pluton)	1320	40	20	1.69	4.93	2.97	1.46	21.2	5.35	4.9	1	18.7	0.44	7.2
10M-10 (Olalla pluton)	2420	25.7	20	0.96	2.03	1.32	0.7	18.7	2.1	2.3	0.43	14.3	0.23	5.5
10M-33 (Mt. Riordan stock)	1350	24.8	30	1.88	2.64	1.67	0.79	17.8	2.67	2.8	0.54	13	0.28	3.8
10KL-111 (Kruger syenite)	932	46.7	10	2.45	2.97	1.71	1.19	18.1	3.53	3.6	0.59	27.5	0.3	9.8
10KL-115 (Bromley batholith)	1580	22	30	2.48	2.73	1.67	0.94	18.3	3	2.3	0.55	10.8	0.25	3.2

Sample	Trace and rare-earth elements (ppm)													
	Nd	Pr	Rb	Sm	Sr	Ta	Tb	Th	Tm	U	V	Y	Yb	Zr
10M-04 (Bromley batholith)	12.1	3.07	64.1	2.86	382	0.3	0.48	3.04	0.3	1.54	148	18.5	1.86	85
10M-05 (Lookout Ridge pluton)	21.1	6.02	140.5	3.9	189.5	0.9	0.52	16.15	0.33	4.07	25	20.3	2.27	152
10M-06 (Toronto stock)	12.7	3.29	80.5	2.99	473	0.3	0.45	4.63	0.26	2.44	166	15.9	1.53	96
10M-07 (Toronto stock)	8	1.9	25.5	1.99	653	0.1	0.33	1.53	0.18	0.78	157	11.1	1.12	45
10M-08 (Cahill Creek pluton)	22.4	5.24	69.2	5.42	469	0.4	0.83	7.06	0.47	2.62	122	29.6	2.86	182
10M-10 (Olalla pluton)	10.7	2.87	113.5	2.21	590	0.4	0.32	4.29	0.21	2.7	105	12.5	1.42	82
10M-33 (Mt. Riordan stock)	11.3	2.89	75.5	2.57	371	0.4	0.43	5.1	0.27	2.18	128	16.3	1.73	91
10KL-111 (Kruger syenite)	18.3	4.99	131.5	3.74	662	0.9	0.5	11.5	0.28	2.62	86	17	1.82	118
10KL-115 (Bromley batholith)	11.4	2.77	79.8	2.88	436	0.2	0.45	2.94	0.26	1.55	174	16.4	1.66	80

Analyses done at ALS Chemex, Vancouver, BC. Major elements determined using ICP-AES methods following lithium-metaborate fusion (ALS analytical package ME-ICP06), and trace and rare-earth elements using ICP-MS methods following lithium-metaborate fusion (ALS analytical package ME-MS81)

On the total alkalis versus silica diagram (Figure 5a) of Le Bas et al. (1986), two samples of the Toronto stock plot as diorite, whereas most of the remaining samples fall in the granodiorite/quartz diorite field. The Lookout Ridge pluton sample yields a granite composition, and the Olalla pluton falls just into the syenite field. All of the samples are subalkaline in composition according to the alkaline-subalkaline discriminant diagram (Figure 5a) of Irvine and Baragar (1971). There is considerably more scatter in the whole-rock geochemical analyses from the Boundary dis-

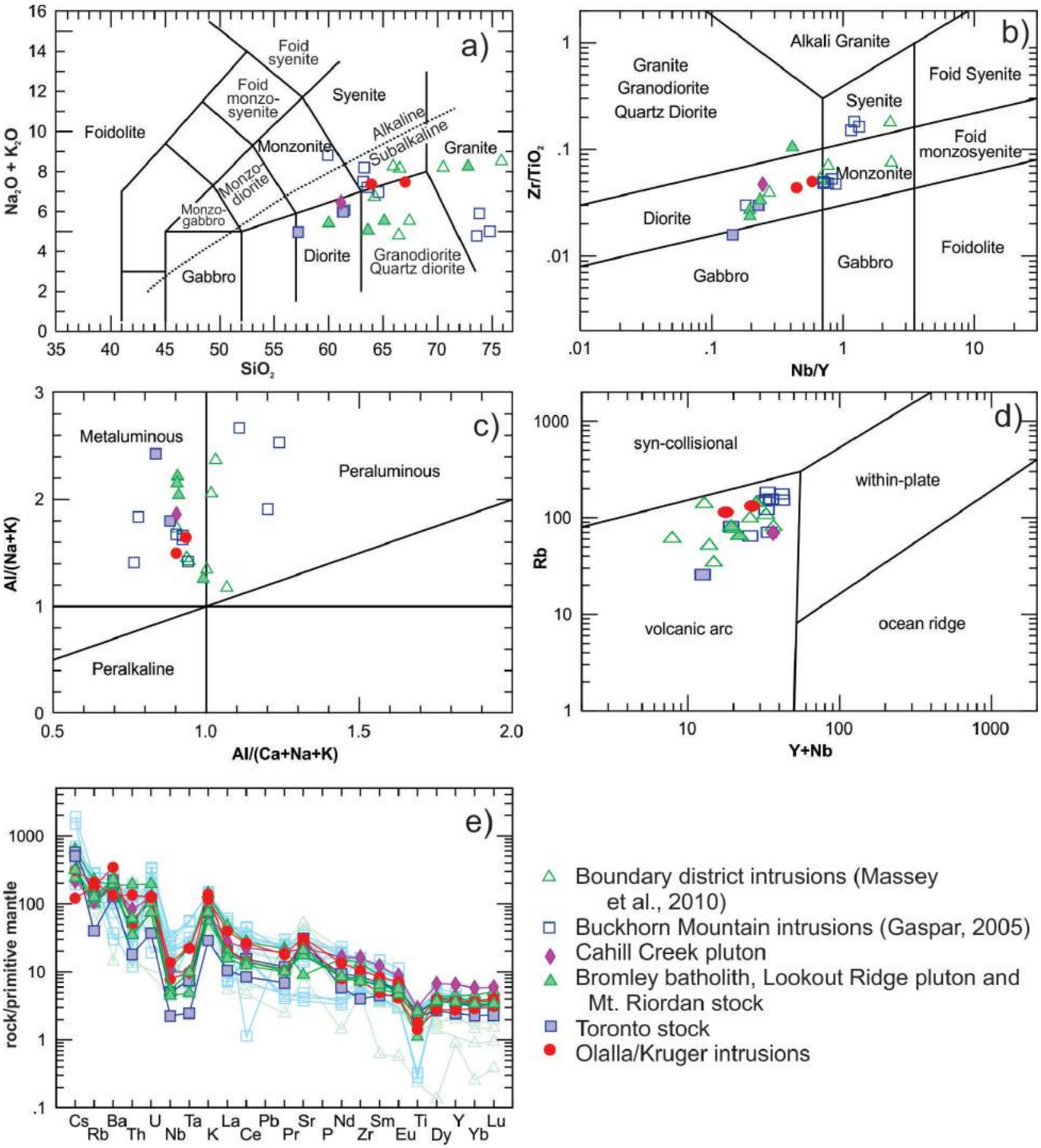

Figure 5. Whole-rock geochemistry of Early and Middle Jurassic intrusive rock units from the Hedley–Apex Mountain area, together with data from intrusions in the Greenwood area (from Massey et al., 2010) and intrusions associated with the Buckhorn Au-bearing skarn in northern Washington state (from Gaspar, 2005). Greenwood and Buckhorn Mountain intrusive samples are shown in pale green and blue symbols, respectively, in part (e). References for the various discriminant plots are **a)** Irvine and Baragar (1971) and Le Bas et al. (1986); **b)** Maniar and Piccoli (1989); **c)** Winchester and Floyd (1977); **d)** Pearce et al. (1984); **e)** Sun and McDonough (1989).

trict and the Buckhorn Mountain area, for which samples ranged from diorite to granite, with several samples plotting well into the syenite field (Figure 5a). Only one of the samples, from the Buckhorn Mountain area, yielded an alkaline composition according to the Irvine and Baragar (1971) discriminant plot.

Samples analyzed in this study fall in a relatively tight cluster on a revised Winchester and Floyd (1977) immobile trace-element ratio plot (Nb/Y versus Zr/TiO_2; Figure 5b). The composition of the Hedley intrusions plots as gabbro to diorite, whereas most of the remaining samples fall in the diorite field, with a single sample plotting slightly into the granite/granodiorite/quartz diorite field. As with the previous plot, much more compositional scatter was displayed by the Jurassic intrusive rocks from the Boundary district (Greenwood area) and Buckhorn Mountain area.

All of the samples from this study fall well within the metaluminous field on a Shand-type plot (Maniar and Piccoli, 1989; Figure 5c). There is much more scatter in the Boundary district and Buckhorn Mountain sample suites, with several samples showing peraluminous compositions. It is unclear whether this represents the original geochemistry or may, in part, be an artifact of superimposed hydrothermal alteration on some of the samples.

All samples from this study, as well as those from the Boundary district and Buckhorn Mountain area, fall within the volcanic-arc field on a Rb versus Y+Nb discriminant plot of Pearce et al. (1984; Figure 5d).

On spider diagrams depicting ratios of high-field-strength and rare-earth element concentrations to primitive-mantle–normalized trace-element values (Sun and McDonough, 1989; Figure 5e), samples from this study show a limited amount of scatter, with all samples characterized by Nb and Ti troughs that are typical of subduction-related magmas. Patterns for samples from the Boundary district and Buckhorn Mountain area are generally similar to those in the study area, although they show a somewhat greater degree of scatter.

Despite their considerable age range, geochemical signatures of Jurassic intrusive rocks in the Hedley–Apex Mountain area, and areas to the east that were investigated in this study, show a surprisingly narrow compositional range. Analyses of the syenite phase of the Olalla pluton and the Kruger syenite showed that, in fact, these bodies are, at best, only weakly alkaline. Combined with geochemical analyses of well-dated igneous rocks from the Boundary district and Buckhorn Mountain area, the new analytical results appear to indicate that Jurassic intrusions in the southern Quesnel terrane of southern BC and adjacent parts of northern Washington state reflect sporadic magmatism within a continental magmatic-arc setting over a period of approximately 40 million years.

Pb-Isotopic Studies of Intrusions and Skarn Mineralization

Lead isotopes can be an effective tool for evaluating the source(s) of metals contained within various styles of mineral deposits. This approach can be particularly useful for intrusion-related mineralization, because one can determine the Pb-isotopic composition of any magmatic fluids that might have been generated during crystallization of the magma by analyzing igneous feldspar (which incorporates significant concentrations of Pb but no U or Th during crystallization, and hence preserves the initial magmatic Pb-isotopic 'signature'). The Pb-isotopic signature can be established for intrusions of various ages and compositions in the study area, and then compared to the Pb-isotopic compositions of sulphides in the mineralization being investigated (as these sulphides also concentrate Pb but little or no U or Th, and thus preserve the isotopic composition from the time of formation). Ideally, there should be a close match between the Pb-isotopic composition of the mineralization and the causative intrusion(s). In the absence of direct-age information for the mineralization, this can provide indirect information regarding the age of mineralization and also identify the specific intrusion, or intrusive suite, that is preferentially associated with the mineralization. However, there are numerous factors that complicate this simple model. Hydrothermal fluids that precipitate sulphides in vein-style mineralization may not interact significantly with wallrocks during fluid flow and therefore commonly (but not always) yield Pb-isotopic compositions that are close to those of the source reservoir(s). However, intrusion-related mineralization that involves a significant amount of wallrock replacement, such as skarns, mantos or high-sulphidation epithermal veins, commonly shows an array of Pb-isotopic compositions that reflects variable mixtures between the magmatic Pb component and Pb derived from the wallrocks themselves. The nature of these mixing arrays depends on several factors, including the Pb contents and extent of compositional ranges between the mineralizing fluids and the wallrocks that are being replaced.

Lead-isotopic compositions were determined for all but one (Olalla pluton) of the intrusive phases that were dated in this study, as well as for a suite of sulphide samples from the Nickel Plate mine and other skarn deposits in the Hedley–Apex Mountain area, and from the Phoenix mine in the Greenwood area. Analytical data are listed in Table 4 and are plotted on $^{208}Pb/^{206}Pb$ versus $^{207}Pb/^{206}Pb$, and $^{207}Pb/^{204}Pb$ versus $^{206}Pb/^{204}Pb$ plots in Figure 6. Two analyses of very scarce galena from the Nickel Plate mine that were reported by Godwin et al. (1988) are also plotted.

Most of the igneous feldspar samples clustered reasonably well on both of the Pb/Pb plots, although several analyses yielded relatively radiogenic compositions, especially in

$^{207}Pb/^{204}Pb$ versus $^{206}Pb/^{204}Pb$ space (Figure 6b). This likely reflects a combination of fractionation error and ^{204}Pb measurement error. This latter source of error is not present in the $^{208}Pb/^{206}Pb$ versus $^{207}Pb/^{206}Pb$ plot (Figure 6a), which shows a tighter clustering of analyses for the igneous feldspar samples. The Toronto stock feldspar analysis is somewhat more radiogenic than most of the other feldspar samples. This may be because this is the only sample for which plagioclase was analyzed rather than K-feldspar (K-feldspar was not present in the sample). Igneous plagioclase typically has substantially lower Pb contents than K-feldspar. Therefore, plagioclase analyses are more susceptible to significant disturbance caused by the addition of even minor amounts of radiogenic Pb resulting from radiogenic ingrowth from minor contained U and/or Th.

Most of the Nickel Plate sulphides (particularly the two galena samples) yielded Pb-isotopic compositions that are close to those from feldspar samples collected in the vicinity of the deposit; however, two of the samples yielded considerably more radiogenic compositions, probably as a result of mixing with radiogenic Pb contained within the hostrocks. All of the sulphides from the Phoenix mine at Greenwood yielded compositions that are substantially more radiogenic than those of feldspar samples from any of the Jurassic intrusions in the region that have been analyzed thus far. There are no likely causative intrusions in the vicinity of the Phoenix skarn deposit, so fluids responsible for forming the skarn may have travelled somewhat farther from the source and/or interacted more extensively with hostrocks containing a higher concentration of radiogenic Pb than in the Hedley–Apex Mountain area. Alternatively, the mineralizing fluids responsible for formation of the Phoenix skarn may have contained lower concentrations of Pb and therefore would have been more strongly modified by mixing of radiogenic Pb from the wallrocks. However, the measured Pb-isotopic compositions of sulphides in the Nickel Plate and Phoenix skarn deposits are consistent, in general, with the deposits having formed through interaction between metalliferous magmatic fluids that evolved from the Jurassic intrusions and various calcareous hostrocks. Unfortunately, the Pb-isotopic compositions of igneous feldspar samples from the various intrusive units were not sufficiently distinct to provide a 'fingerprint' that could be used to determine which intrusion (or intrusive suite) was genetically related to the mineralization.

Table 4. Results of Pb-isotopic analyses for intrusive rock units from the Hedley–Apex Mountain area and sulphide minerals from the Nickel Plate mine (Hedley-Apex Mountain area) and Phoenix mine (Greenwood area).

Sample no.	Mineral	Occurrence	Source	$^{208}Pb/^{204}Pb$	1σ (%)
Hedley-1	Arsenopyrite+pyrite	Disseminated sulphides in massive diopside-garnet skarn, Hedley north pit	1	19.172	0.08
Hedley-2	Pyrrhotite	Disseminated and vein sulphides in massive diopside skarn, Hedley glory hole	1	18.785	0.04
Hedley-Sunny-side-1	Arsenopyrite	Massive arsenopyrite in skarn, Sunnyside deposit	1	18.710	0.03
Hedley-Sunny-side-2	Arsenopyrite	Massive arsenopyrite in skarn, Sunnyside deposit	1	18.782	0.01
Hedley-2-8N stope	Arsenopyrite	Massive arsenopyrite, Hedley 8N stope	1	18.928	0.04
Phoenix-1	Chalcopyrite+pyrite	Lower ore zone	1	19.207	0.06
Phoenix-2	Chalcopyrite	Chalcopyrite in quartz, southeast end of open pit	1	19.251	0.08
Phoenix-3	Chalcopyrite	Chalcopyrite-hematite-quartz ore	1	22.022	0.05
Phoenix-4	Pyrite	High-grade skarn	1	19.207	0.02
Phoenix-5	Chalcopyrite	High-grade skarn	1	19.468	0.01
Phoenix-6	Pyrite	Upper ore zone, east side of Phoenix open pit	1	19.000	0.01
30302-002 *	Galena	Nickel Plate skarn	2	18.724	0.01
30302-003 *	Galena	Nickel Plate skarn	2	18.731	0.03
10-M-07	Feldspar	Offshoot of Toronto stock	3	19.001	0.35
10-M-06	Feldspar	Offshoot of Toronto stock	3	18.970	0.05
10-M-04	Feldspar	Bromley batholith	3	18.807	0.28
10-M-05	Feldspar	Lookout Ridge pluton	3	18.731	0.03
10-M-05	Feldspar	Lookout Ridge pluton	3	18.782	0.01
10-M-33	Feldspar	Mount Riordan pluton	3	18.736	0
10KL-115	Feldspar	Bromley batholith?	3	19.184	0.09
10KL-115 (repl.)	Feldspar	Bromley batholith?	3	18.712	0.12
10-M-08	Feldspar	Cahill Creek stock	3	18.729	0.04
10KL-111	Feldspar	Kruger syenite	3	18.711	0.01
10-M-10	Feldspar	Olalla pluton	3	19.081	0.3

Sample and data sources: 1, University of British Columbia mineral deposit sample collection (exact locations uncertain); 2, Godwin et al. (1988); 3, this study.

Implications for Timing of Magmatism and Skarn Formation in the Southern Quesnel Terrane

Results of this study, together with those of previous work done in the Boundary Creek mineral district by Massey et al. (2010) and the Buckhorn Mountain area by Gaspar (2005) and Scorrar (2012), demonstrate that magmatism in this part of the southern Quesnel terrane occurred sporadically over an extended period of at least 40 m.y. (from ca. 197 to 157 Ma). Geochemical compositions of these intrusions are consistent with all of this magmatism having occurred within a continental or continental-margin volcanic-arc setting. The Jurassic intrusions were emplaced into an older arc assemblage (the Nicola Group), which itself was built on middle and late Paleozoic metasedimentary and metavolcanic basement rocks. The age of the formation of Au and Au-Cu skarn mineralization in the Hedley–Apex Mountain area and the Boundary district remains unresolved by direct dating methods. Scorrar (2012) has shown that the Buckhorn Au skarn in the Buckhorn Mountain area formed between 168 and 162 Ma. Although there are close similarities between the Buckhorn skarn and deposits in the Hedley area, Ray et al. (1996) provided compelling evidence, based on field observations in the Hedley area, that skarn deposits there are considerably older than the Buckhorn deposit and are likely related to the 196 Ma Toronto stock. It is unclear whether the Mount Riordan garnet skarn (Figure 2) formed at the same time as the better-studied Au skarns in the area. Developing a more robust exploration model for new Au-Cu skarn deposits in this area will require further work in both the Hedley and Boundary Creek mineral district areas to better constrain the age of the skarns and identify the specific intrusive events with which the skarn deposits are associated.

Acknowledgments

This project was funded by Geoscience BC. The author thanks J. Monger and K. Lucas for their assistance with sample collection, and M. Allan, who provided a review of an earlier version of the manuscript.

References

BC Geological Survey 2013: MINFILE BC mineral deposits database; BC Ministry of Energy and Mines, BC Geological Survey, URL <http://minfile.ca/> [November 2013].

Beranek, L.P. and Mortensen, J.K. (2011): The timing and provenance record of the Late Permian Klondike orogeny in

Table 4 (continued)

Sample no.	$^{207}Pb/^{204}Pb$	1σ (%)	$^{206}Pb/^{204}Pb$	1σ (%)	$^{208}Pb/^{206}Pb$	1σ (%)	$^{207}Pb/^{206}Pb$	1σ (%)
Hedley-1	15.656	0.08	38.446	0.08	0.8166	0.007	2.0053	0.002
Hedley-2	15.613	0.04	38.395	0.04	0.8311	0.009	2.0440	0.005
Hedley-Sunny-side-1	15.606	0.02	38.404	0.03	0.8341	0.005	2.0526	0.004
Hedley-Sunny-side-2	15.615	0.01	38.391	0.01	0.8313	0.006	2.0440	0.005
Hedley-2-8N stope	15.613	0.04	38.391	0.04	0.8248	0.006	2.0282	0.007
Phoenix-1	15.655	0.06	38.652	0.06	0.8151	0.007	2.0124	0.006
Phoenix-2	15.576	0.08	38.415	0.08	0.8091	0.019	1.9955	0.010
Phoenix-3	15.791	0.05	38.675	0.05	0.7170	0.012	1.7562	0.013
Phoenix-4	15.682	0.02	38.918	0.02	0.8165	0.010	2.0262	0.008
Phoenix-5	15.625	0.01	38.407	0.01	0.8026	0.005	1.9729	0.008
Phoenix-6	15.647	0.01	38.523	0.01	0.8235	0.001	2.0275	0.002
30302-002 *	15.605	0.02	38.354	0.02	0.8334	0.01	2.0485	0.01
30302-003 *	15.607	0.03	38.368	0.04	0.8332	0.01	2.0483	0.01
10-M-07	15.553	0.21	38.858	0.47	0.8186	0.28	2.0451	0.311
10-M-06	15.692	0.05	38.667	0.05	0.8272	0.019	2.0383	0.02
10-M-04	15.652	0.28	38.507	0.28	0.8323	0.04	2.0475	0.03
10-M-05	15.578	0.03	38.356	0.03	0.8317	0.007	2.0478	0.003
10-M-05	15.632	0	38.511	0.01	0.8323	0.003	2.0505	0.002
10-M-33	15.601	0	38.383	0	0.8326	0.001	2.0486	0.002
10KL-115	15.631	0.09	38.678	0.09	0.8148	0.013	2.0162	0.012
10KL-115 (repl.)	15.694	0.12	38.484	0.12	0.8387	0.015	2.0566	0.019
10-M-08	15.609	0.04	38.406	0.04	0.8334	0.01	2.0506	0.011
10KL-111	15.585	0	38.339	0.01	0.8329	0.002	2.049	0.001
10-M-10	15.531	0.29	38.435	0.31	0.8139	0.061	2.0143	0.068

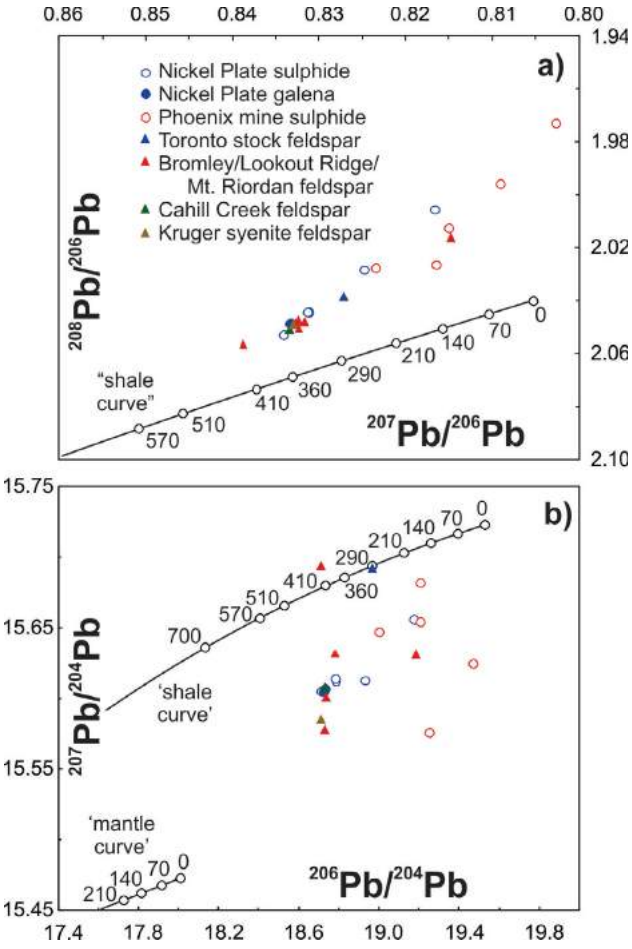

Figure 6. Lead-isotopic compositions for sulphide minerals from the Nickel Plate mine in the Hedley–Apex Mountain area and the Phoenix mine in the Greenwood area, as well as for igneous feldspar samples from dated Early and Middle Jurassic intrusive rocks in the Hedley–Apex Mountain area and the Kruger syenite. Analyses of galena from the Nickel Plate mine are from Godwin et al. (1988). The 'shale curve' is a model growth curve for the evolution of Pb-isotopic compositions in the miogeocline of the North American Cordillera (from Godwin and Sinclair, 1982). The 'mantle curve' is a model growth curve for Pb-isotopic evolution in the mantle (from Doe and Zartman, 1979).

northwestern Canada and arc-continent collision along western North America; Tectonics, v. 30, p. TC5017.

Bostock, H.S. (1940): Geology, Olalla; Geological Survey of Canada, Map 628A, scale 1:63 360.

Doe, B.R. and Zartman, R.E. (1979): Plumbotectonics, the Phanerozoic; *in* Geochemistry of Hydrothermal Ore Deposits (Second Edition), H.L. Barnes (ed.), John Wiley and Sons, p. 22–70.

Ettlinger, A.D., Meinert, L.D. and Ray, G.E. (1992): Skarn evolution and hydrothermal fluid characteristics in the Nickel Plate deposit, Hedley district, British Columbia; Economic Geology, v. 87, p. 1541–1565.

Gaspar, L.M.G. (2005): The Crown Jewel gold skarn deposit; unpublished Ph.D. thesis, Washington State University, 325 p.

Godwin, C.I. and Sinclair, A.J. (1982): Average lead isotope growth curves for shale-hosted zinc-lead deposits, Canadian Cordillera; Economic Geology, v. 77, p. 675–690.

Godwin, C.I., Gabites, J.E. and Andrew, A. (1988): Leadtable—a galena lead isotope database for the Canadian Cordillera, with a guide to its use by explorationists; BC Ministry of Energy and Mines, Geological Survey Branch, Paper 1988-4, 188 p.

Irvine, T.N. and Baragar, W.R.A. (1971): A guide to the chemical classification of the common volcanic rocks; Canadian Journal of Earth Sciences, v. 8, p. 523–548.

Le Bas, M.J., Le Maitre, R.W., Streckeisen, A. and Zanettin, B. (1986): A chemical classification of volcanic rocks based on the total alkali-silica diagram; Journal of Petrology, v. 27, p. 745–750.

Maniar, P.D. and Piccoli, P.M. (1989): Tectonic discrimination of granitoids; Geological Society of America, Bulletin, v. 101, p. 635–643.

Massey, N.W.D., Gabites, J.E., Mortensen, J.K. and Ullrich, T.D. (2010): Boundary Project: geochronology and geochemistry of Jurassic and Eocene intrusions, southern British Columbia (NTS 082E); *in* Geological Fieldwork 2009, BC Ministry of Energy and Mines, BC Geological Survey, Paper 2010-1, p. 1–16.

Mortensen, J.K., Lucas, K., Monger, J.W.H. and Cordey, F. (2011): Geological investigations of the basement of the Quesnel terrane in southern British Columbia (NTS 082E, F, L, 092H, I): progress Report; *in* Geoscience BC Summary of Activities 2010, Report 2011-1, p. 133–142.

Pearce, J.A., Harris, N.B.W. and Tindle, A.G. (1984): Trace element discrimination diagrams for the tectonic interpretation of granitic rocks; Journal of Petrology, v. 25, p. 956–983.

Ray, G.E. and Dawson, G.L. (1994): The geology and mineral deposits of the Hedley gold skarn district, southern British Columbia; BC Ministry of Energy and Mines, BC Geological Survey, Bulletin 87, 156 p.

Ray, G.E., Dawson, G.L. and Webster, I.C.L. (1996): The stratigraphy of the Nicola Group in the Hedley district, British Columbia, and the chemistry of its intrusions and Au skarns; Canadian Journal of Earth Sciences, v. 33, p. 1105–1126.

Scorrar, B.A. (2012): The age and character of alteration and mineralization at the Buckhorn gold skarn, Okanogan County, Washington, USA; M.Sc. thesis, University of British Columbia, 204 p.

Sun, S.S. and McDonough, W.F. (1989): Chemical and isotopic systematics of oceanic basalts: implications for mantle composition and processes; *in* Magmatism in the Ocean Basins, A.D. Saunders and M.J. Norry (ed.), Geological Society, Special Publication 42, p. 313–345.

Tafti, R., Mortensen, J.K., Lang, J.R., Rebagliati, M., and Oliver, J.L. (2009): Jurassic U-Pb and Re-Os ages for the newly discovered Xietongmen Cu-Au porphyry district, Tibet, PRC: implications for metallogenic epochs in the southern Gangdese belt; Economic Geology, v. 104, p. 127–136.

Winchester, J.A. and Floyd, P.A. (1977): Geochemical discrimination of different magma series and their differentiation products using immobile elements; Chemical Geology, v. 20, p. 325–343.